Geophysical Journal International

Geophys. J. Int. (2014) **196,** 918–923
Advance Access publication 2013 November 11

doi: 10.1093/gji/ggt404

A new hybrid Coulomb/statistical model for forecasting aftershock rates

Sandy Steacy,[1] Matt Gerstenberger,[2] Charles Williams,[2] David Rhoades[2] and Annemarie Christophersen[2]

[1]*School of Environmental Sciences, University of Ulster, Cromore Road, Coleraine,* BT52 1SA, *Northern Ireland. E-mail:* s.steacy@ulster.ac.uk
[2]*GNS Science,* 1 *Fairway Drive, P.O. Box* 30368, *Lower Hutt, New Zealand*

Accepted 2013 October 1. Received 2013 September 30; in original form 2013 July 28

SUMMARY

Forecasting the spatial and temporal distribution of aftershocks is of great importance to earthquake scientists, civil protection authorities and the general public as these events cause disproportionate damage and consternation relative to their size. At present, there are two main approaches to such forecasts—purely statistical methods based on observations of the initial portions of aftershock sequences and a physics-based approach based on Coulomb stress changes caused by the main shock. Here we develop a new method which combines the spatial constraints from the Coulomb model with the statistical power of the STEP (short-term earthquake probability) approach. We test this pseudo prospectively and retrospectively on the Canterbury sequence against the STEP model and a Coulomb rate–state method, using data from the first 10 d following each main event to forecast the rate of $M \geq 4$ events in the following 100 d. We find that in retrospective tests the new model outperforms STEP for two events in the sequence but this is not the case for pseudo-prospective tests. Further, the Coulomb rate–state approach never performs better than STEP. Our results suggest that incorporating the physical constraints from Coulomb stress changes can increase the forecasting power of statistical models and clearly show the importance of good data quality if prospective forecasts are to be implemented in practice.

Key words: Probabilistic forecasting; Earthquake interaction, forecasting, and prediction; Statistical seismology.

1 INTRODUCTION

There are two main statistical approaches to aftershock forecasting, the ETAS (epidemic-type aftershock sequence, e.g. Ogata 1988; Ogata & Zhuang 2006) and short-term earthquake probability (STEP; Gerstenberger *et al.* 2005) models. Both rely on two fundamental observations in seismology, the Gutenberg–Richter relation and the Omori Utsu law. In the ETAS model every earthquake is a main shock with its own aftershock sequence and the rate of earthquake occurrence depends on the background seismicity rate and the productivity of each main shock in terms of triggering aftershocks (Ogata 1988).

The STEP model (Gerstenberger *et al.* 2005) is also based on superimposed Omori sequences, where every earthquake is allowed to generate its own aftershock sequence. A forecast is created using an ensemble of three different models of increasing complexity, which are combined using weights calculated from the Akaike Information Criterion (Burnham & Anderson 2002). Spatially, the ensemble forecast is typically dominated by the most simple model which is based on STEP parameters from the historical catalogue. For this component of the ensemble forecast, a fault is estimated from the observed aftershock distribution and the forecast rates are isotropically smoothed away from the fault using a $1/r^2$ taper. Spatial heterogeneity is then added to the forecast using parameters that are estimated based on the ongoing sequence.

In contrast, the Coulomb method is a physics-based approach, which calculates the static stress changes due to earthquake slip in the nearby region. These stress changes have been shown by a number of authors to influence the spatial distribution of subsequent events and, in particular, aftershocks tend to occur in areas where the Coulomb stress has been increased due to main shock rupture (see Steacy *et al.* 2005, for a review). Potential rate changes due to Coulomb stress perturbations are generally computed through a rate–state formulation based on laboratory friction models (Dieterich 1994; Parsons *et al.* 2000; Toda *et al.* 2005). The key experimental observation is that friction is an acceleration to failure process and hence, with the assumption of a uniform population of future nucleation sites, the Dieterich formulation (1994) allows computation of the expected rate of seismicity for a given stress change and background rate.

One limitation of the Coulomb rate–state approach is its dependence on poorly defined parameters such as background loading rate, aftershock decay rate and a constitutive parameter (Hainzl *et al.* 2010). Additionally, the forecast aftershock rate is strongly dependent on the magnitude of the stress change at any location (Dieterich 1994; Hainzl *et al.* 2009) and this, in turn, depends directly on knowledge of the detailed slip distribution of the causative event (Steacy *et al.* 2004). However, it is quite common for several very different slip models to be published after any particular event and these can lead to very different forecasts (Hainzl *et al.* 2009).

Here we develop a new method for forecasting aftershock rates, which combines the statistical approach of the STEP model with the spatial constraints provided by the Coulomb stress changes. We apply the new model to the Canterbury earthquake sequence and test it against the New Zealand application of the STEP model and an implementation of the Coulomb rate–state model (C-RS). Since 2010, the Canterbury region has experienced four significant earthquakes that migrated from west to east—in order these are the $M_w = 7.1$ Darfield event of 2010 September 4, the $M_w = 6.2$ Christchurch earthquake of 2011 February 22, a further $M_w = 6.0$ event on 2011 June 13 and $M_w = 5.8$ and 5.9 events on 2011 December 23.

2 METHOD

We avoid the problems associated with accurate calculation of stress change magnitudes by treating the stress field as a Boolean and modifying STEP forecasts based purely on the computed pattern of positive/negative stress. Specifically, we run the STEP model as our base but redistribute forecast rates so the 93 per cent of events are expected to occur in positively stressed regions; this value comes from our observations of the correlation between positive stress and aftershocks in several California sequences (so in essence it's a generic parameter). We investigate two variations of this model, one (STEPC1) in which we apply the STEP model within 5 km of the fault zone but redistribute rates away from it; the other (STEPC2) in which we apply the Coulomb-based redistribution everywhere.

We compute the Coulomb stress patterns by resolving the tensorial stress perturbation onto 3-D optimally oriented planes at a depth of 7.5 km assuming an effective coefficient of friction of 0.4. We use regional horizontal stress orientations of $\sigma_1 = 115^\circ$, $\sigma_3 = 25^\circ$ with σ_2 vertical (Sibson *et al.* 2011), and assume compressive stress values of $\sigma_1 = 10$ MPa, $\sigma_2 = 0.5$ MPa and $\sigma_3 = 0.1$ MPa; the near equal values of the latter are consistent with observations of both strike-slip and reverse faulting in the region (Sibson *et al.* 2011). The stress values are consistent with the literature (e.g. Toda *et al.* 2005) and have been used throughout this study without any attempt at optimization. The calculations are done for an elastic half-space and we assume that the Lame constants (λ and μ) are each equal to 3×10^4 MPa

The slip models for the pseudo-prospective tests ('10 d') were provided to us by Caroline Holden (personal communication, 2012) as she has a record of the dates on which each preliminary model was computed. For the retrospective tests, we chose the six-fault model of Beavan *et al.* (2012) for the Darfield earthquake, for the February event, we use the source model of Holden (2011) and for the June and December earthquakes we use the source models described in Holden & Beavan (2012).

In the Coulomb rate–state model, we calculate seismicity rate changes using the method of Catalli *et al.* (2008) which computes the reference shear stressing rate from the reference seismicity rate and apply the Dieterich formulation (1994) to compute the response of the seismicity rate to sudden stress steps. (See Supporting Information for more details.) We compute the reference seismicity rate using the Proximity to Past Earthquakes (PPE) smoothed seismicity model as implemented by Rhoades & Evison (2004). The reference model smooths the locations of earthquakes with magnitude $M \geq 4.0$ from 1964 January 1 to 2011 September 3 (just prior to the Darfield main shock) using an inverse power-law smoothing kernel and weighting all earthquakes equally. All calculations and tests are performed on a $0.05^\circ \times 0.05^\circ$ grid.

3 RESULTS

We test the models by using the first 10 d of data after each event to forecast the rates of $M \geq 4$ aftershocks in the subsequent 100 d. We do this both retrospectively using currently available data and pseudo-prospectively based on the data actually available at the time. For the latter, we ensure that we only use slip models that would have been available within the first 10 d; for instance for the Darfield event this slip model was a single approximately E–W striking fault plane with primarily right lateral displacement. By contrast, a later more sophisticated model incorporating GPS and InSAR data contained six faults—including two with primarily thrust motion (Beavan *et al.* 2012). Note that this model is used in the pseudo-prospective forecasts for the later events because it was available in 2010 November, well within the learning periods for the 2011 forecasts.

The pseudo-prospective forecasts following the Darfield earthquake are shown in Fig. 1. The Coulomb pattern is clearly evident in the STEPC models with areas of higher forecast rate corresponding to regions of positive Coulomb stress, and lower rates in negative stress locations. Both STEPC models have greater near fault forecast rates than STEP as a result of the positive Coulomb stress adjacent to the fault zone; the on-fault rates in STEPC2 are the highest of the three models because of the superposition of the STEP $1/r^2$ taper and the Coulomb-based rate redistribution.

The forecast rates from the Coulomb rate–state model are very different from the STEP-derived approaches. The overall forecast rate is generally less (Table 1) because the background rate is very low as the Canterbury Plain experienced little seismicity prior to the Darfield event. Additionally, the large negative stress drops close to the fault zone lead to some very low forecast rates, for instance three $M > 4$ aftershocks occurred in locations where the forecast rate is less than 10^{-14}.

The dependence of the Coulomb stress pattern (and the forecast rates) on the slip model is apparent from comparison with Fig. 2 where we plot the forecast rates for the retrospective models. Here the northerly lobe of Coulomb stress is rotated to the east because the six-fault slip model contains the NE-striking Charing Cross thrust fault north of the main E–W fault plane. The total forecast rate for the STEP models is slightly higher due to the greater number of events in the retrospective catalogue used in the learning period.

The Coulomb rate–state model shows the greatest change with much higher forecast rates in the northerly lobe of positive stress and adjacent to the fault zone. The former results from higher stress magnitudes in that region and the latter is due to an increased area of positive stress due to the additional faults. With the retrospective slip distribution the total forecast rate is 47.4 (quite close to the observed value of 49), whereas for this pseudo-prospective model the total rate was only 28.7. Note that both the pseudo-prospective and retrospective STEP models significantly overestimate the rate.

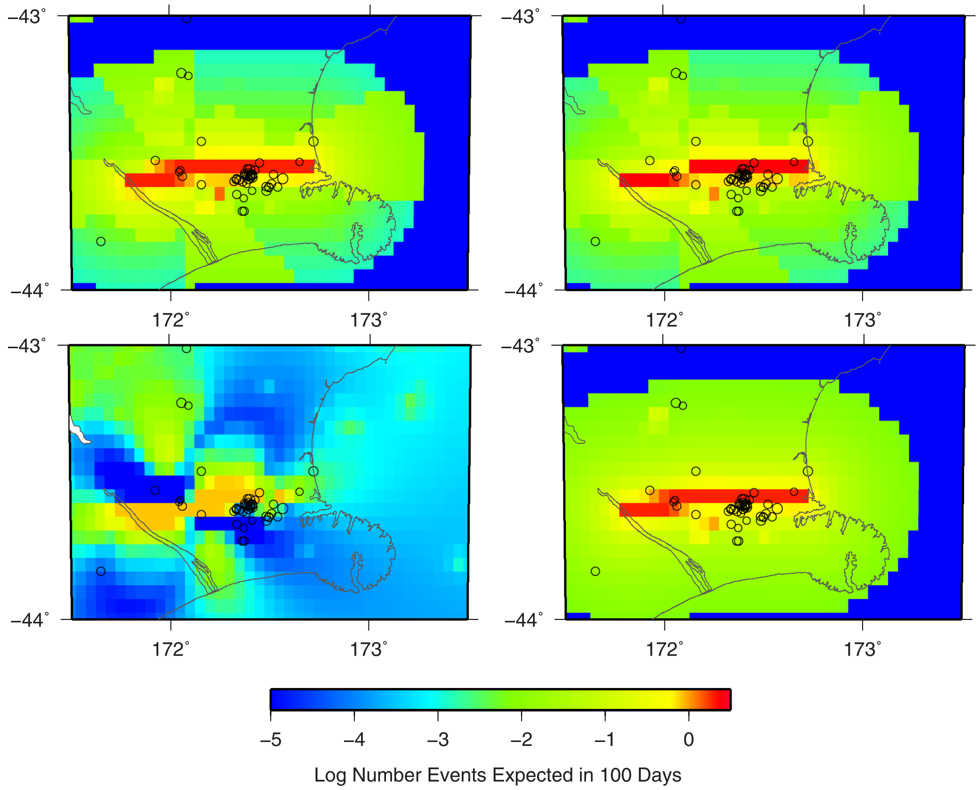

Figure 1. Forecast rates following the Darfield earthquake for the four pseudo-prospective models. From left to right, top to bottom, these are STEPC1 (with STEP on the fault zone), STEPC2 (applying the Coulomb filter everywhere), Coulomb rate–state and STEP. Open circles indicate the epicentres of the $M \geq 4$ aftershocks that occurred in the 100-d testing period.

Table 1. Observed and forecast number of $M \geq 4$ aftershocks in each 100-d testing period. The abbreviation ‘pp’ indicates results for pseudo-prospective tests and ‘r’ stands for retrospective. The forecast number of events for the STEPC models is the same as for STEP since the Coulomb filter simply redistributes rate.

	Darfield	February	June	December
Observed	49	30	24	27
STEP_pp	76.9	22.7	22	15.6
C-RS_pp	28.7	16.4	16.6	16.5
STEP_r	78.4	22.7	27	20.8
C-RS_r	47.4	21.4	18.8	16.0

(The pseudo-prospective and retrospective forecasts for the later sequences are shown in Figs S1–S6.)

In Table 2, we compare the STEPC and Coulomb rate–state models to STEP for each earthquake and input data set using a t-test which measures the significance of the information gain per earthquake (IGPE) of one model over another (Rhoades *et al.* 2011). The IGPE is the increase in the log-likelihood divided by the number of earthquakes; a 95 per cent confidence interval for the IGPE that does not include zero indicates a significant difference in the information value of the two models.

Our first observation is that the pseudo-prospective Coulomb rate–state models always perform significantly worse than STEP and its derivatives, although the model performance compared to STEP improves with later events. The same pattern is observed for the retrospective tests, with the model performance for the first three events worse than STEP but with improvement to equivalent within confidence limits for the December test.

The comparison between the STEPC models and STEP is more complicated. For the pseudo-prospective tests, the new models perform worse than STEP for the Darfield and December sequences and the same within confidence limits for the February and June ones. However, with the more developed slip models, both perform equally well as STEP for the September and February sequences and better for December. For the June sequence, both models perform better than STEP but only STEPC1 (where STEP is applied along the fault zone) does so when confidence limits are considered. [Note that we also computed a modified version of the s-test (Zechar *et al.* 2010), using a log-likelihood function, which ignores the discretization of space into cells (Rhoades *et al.* 2011), and found that all models, including C-RS, are consistent with the data.]

4 DISCUSSION AND CONCLUSIONS

The results are strongly dependent on the accuracy of the slip model and this is clear from comparisons between the different retrospective forecasts as well as between pseudo-prospective and retrospective ones. In the case of Darfield, for instance, the original slip distribution (a single E–W plane) is very different from the one used subsequently (six faults, three with NE/SW orientations) and this may explain why all the Coulomb models perform worse than STEP which is independent of externally derived slip distributions. The improvement in the retrospective tests is likely due to the use of a more accurate slip model, however the better performance of the STEP model may suggest that the six-fault model does not fully capture the complexity of the Darfield rupture.

We test this retrospectively using two other sets of slip models, one obtained by Atzori *et al.* (2012) who modelled the Darfield,

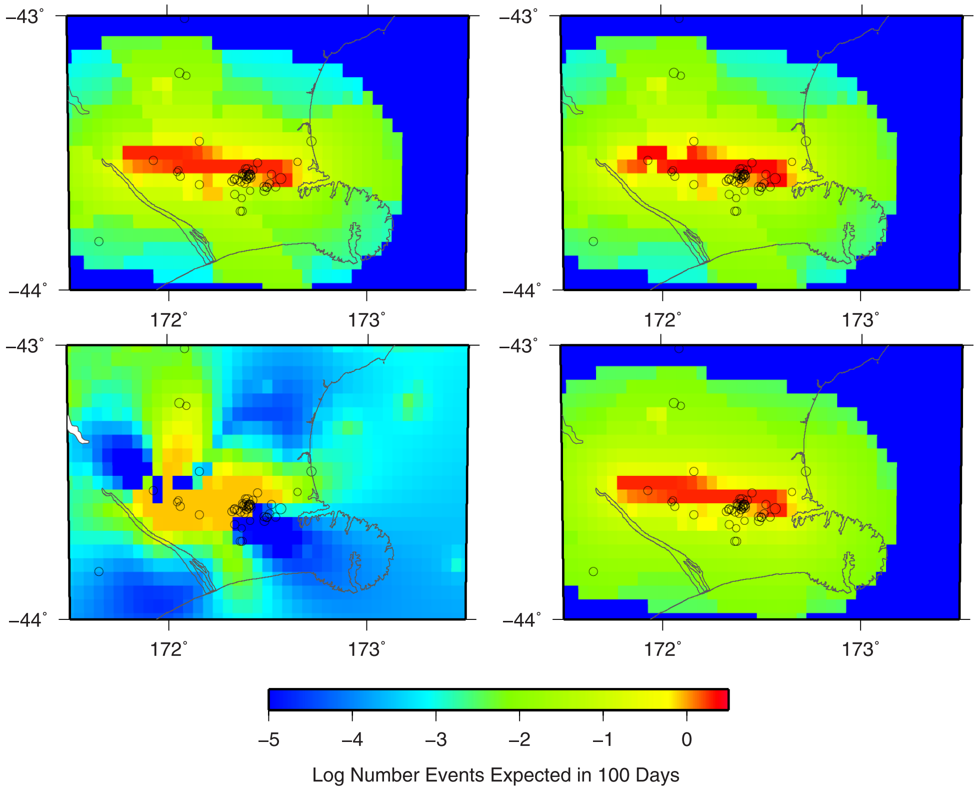

Figure 2. Forecast rates following the Darfield earthquake for the four retrospective models. From left to right, top to bottom, these are STEPC1, STEPC2, Coulomb rate–state and STEP. Open circles indicate the epicentres of the $M \geq 4$ aftershocks that occurred in the 100-d testing period.

Table 2. Results of the *t*-tests for information gain per earthquake (IGPE) for the various models and input data sets. The set on the left is for the pseudo-prospective tests whereas the one on the right is for the retrospective ones. Each model is compared to the STEP model (with the same input data); negative values with confidence limits less than the IGPE (shown in red) indicate models that perform better than STEP whereas positive values with confidence limits less than the IGPE (blue) indicate models that do worse. Values that, within confidence limits, range from negative to positive are shown in green and indicate that within error the models perform as well as STEP; bold type indicates those for which the IGPE is better than for STEP.

	STEPC1_pp	STEPC2_pp	C-RS_pp	STEPC1_r	STEPC2_r	C-RS_r
Darfield						
IG/eq	0.2622	0.1818	6.3159	0.1563	0.0720	3.0271
Confidence	0.2010	0.1792	2.4660	0.1697	0.1418	2.0955
February						
IG/eq	**−0.0176**	**−0.0185**	1.3344	**−0.0411**	**−0.0324**	0.9494
Confidence	0.0674	0.0250	0.8286	0.0880	0.0379	0.9524
June						
IG/eq	0.0240	0.0436	2.7055	−0.0721	**−0.0767**	2.0584
Confidence	0.1012	0.0951	1.6415	0.0484	0.1667	2.0813
December						
IG/eq	0.0027	0.0185	0.4388	−0.0337	−0.0227	0.2390
Confidence	0.0003	0.0001	0.5060	0.0093	0.0001	0.5028

Christchurch, and June events and found that the Darfield earthquake involved eight rupture planes, the Christchurch event two and the June earthquake one; and the other from Elliott *et al*. (2012) who modelled the Darfield and Christchurch events and also found eight and two rupture planes, respectively. The results are shown in Table 3, the majority of these Coulomb-based models perform better with respect to STEP than those derived from the six-fault Darfield slip model of Beavan *et al*. (2012). This suggests that the slip models with eight rupture planes may better describe the complex Darfield rupture; this is in line with observations by Steacy *et al*. (2013) that a greater percentage of aftershocks are consistent with Coulomb triggering for stress maps computed using these slip models compared to the one of Beavan *et al*. (2012).

The differences between the initial and final forecasts of the Coulomb-based models for the February earthquake are much less, probably because the same slip model is used for Darfield and the

Table 3. Results of the *t*-tests for information gain per earthquake (IGPE) for retrospective tests using the slip models developed by Atzori *et al*. (2012) (Atz) and Elliott *et al*. (2012) (Ell). The colour coding is the same as in Table 2 and there are no June results for Elliott *et al*. because the authors did not model the slip in that earthquake.

	STEPC1_Atz	STEPC2_Atz	C-RS_Atz	STEPC1_Ell	STEPC2_Ell	C-RS_Ell
Darfield						
IG/eq	0.0554	0.0051	1.4523	0.0295	**−0.0002**	0.6918
Confidence	0.1213	0.0588	2.0874	0.0965	0.0011	1.1858
February						
IG/eq	−0.0760	−0.0200	0.2917	0.0066	**−0.0074**	0.7691
Confidence	0.0219	0.0001	0.3976	0.1025	0.0387	0.8668
June						
IG/eq	−0.0503	**−0.0810**	0.9863			
Confidence	0.0332	0.0922	1.3008			

difference between the slip models used for the February event is relatively small. However, we note that both STEPC models perform better than STEP in retrospective tests for forecasts built on the slip models of Atzori *et al.* (2012). By contrast, the initial slip model for June contained one fault plane whereas the one used in the retrospective forecast has two; this may explain the larger differences between the forecasts and also the poorer performance for June compared to February of all the Coulomb-based models in the pseudo-prospective tests. The effect of the slip model on the results is strongest for the Coulomb rate–state model because the forecasts depend on the magnitude of the stress change, not just the sign. In addition, the STEP-derived models have an advantage over the Coulomb rate–state one as they include seismicity information from the learning periods which is not considered in C-RS.

Our results suggest that including spatial constraints from Coulomb stress changes can increase forecasting power when good data are available. This is consistent with the one prior study of a hybrid model in which Bach & Hainzl (2012) retrospectively tested a combined Coulomb/ETAS model for three California earthquakes and found that the addition of the Coulomb information improved forecasts of off-fault aftershock locations.

Additionally, our results suggest that these hybrid models which combine stress patterns with statistical techniques may be more appropriate than those based on the Coulomb rate–state method. We believe that this is the first (even pseudo) prospective test of the Coulomb rate–state model and the results are consistent with work by Woessner *et al*. (2011) who compared a set of statistical and Coulomb models in a forward looking retrospective test on the Landers earthquake; the parameters could not be altered but the Coulomb modellers had access to a slip model published 2 yr after the event. They found that the statistical models generally performed better than Coulomb rate–state; no hybrid models such as the ones presented here were tested.

Finally we find that good data quality is crucial, particularly the robustness of the slip inversions, and we suggest that this must be considered carefully before prospective forecasts are put in the public domain.

ACKNOWLEDGEMENTS

We thank two anonymous reviewers for constructive comments which improved the manuscript, as well as the Editor, Jeannot Trampert, for handling it efficiently. We also thank Caroline Holden for providing us with unpublished slip distributions and colleagues at GNS Science for data and support. We acknowledge the New Zealand GeoNet project and its sponsors EQC and GNS Science for providing earthquake data used in the study. This work received financial support from GNS Science, the Natural Environment Research Council, the Leverhulme Trust and the EC FP7 program (contract # 282862) as part of the Strategies and tools for Real-Time Earthquake Risk Reduction (REAKT) project.

REFERENCES

Atzori, S., Tolomei, C., Antonioli, A., Merryman Boncori, J.P., Bannister, S., Trasatti, E., Pasquali, P. & Salvi, S., 2012. The 2010–2011 Canterbury, New Zealand, seismic sequence: multiple source analysis from InSAR data and modeling, *J. geophys. Res.,* **117,** B08305, doi:10.1029/2012JB009178.

Bach, C. & Hainzl, S., 2012. Improving empirical aftershock modeling based on additional source information, *J. geophys. Res.,* **117,** B04312, doi:10.1029/2011JB008901.

Beavan, J., Motagh, M., Fielding, E., Donnelly, N. & Collett, D., 2012. Fault slip models of the 2010–2011 Canterbury, New Zealand, earthquakes from geodetic data, and observations of post-seismic ground deformation, *N. Z. J. Geol. Geophys.,* **55,** 207–221.

Burnham, K.P. & Anderson, D.R., 2002. *Model Selection and Multimodel Inference, A Practical Information-Theoretic Approach,* Springer-Verlag.

Catalli, F., Cocco, M., Console, R. & Chiaraluce, L., 2008. Modeling seismicity rate changes during the 1997 Umbria-Marche sequence (central Italy) through a rate- and state-dependent model, *J. geophys. Res.,* **113,** B11301, doi:10.1029/2007JB005356.

Dieterich, J.H., 1994. A constitutive law for rate of earthquake production and its application to earthquake clustering, *J. geophys. Res.,* **99,** 2601–2618.

Elliott, J.R., Nissen, E.K., England, P.C., Jackson, J.A., Lamb, S., Li, Z., Oehlers, M. & Parsons, B., 2012. Slip in the 2010–2011 Canterbury earthquakes, New Zealand, *J. geophys. Res.,* **117,** B03401, doi:10.1029/2011JB008868.

Gerstenberger, M.C., Wiemer, S., Jones, L.M. & Reasenberg, P.A., 2005. Real-time forecasts of tomorrow's earthquakes in California, *Nature,* **435,** 328–331.

Hainzl, S., Enescu, B., Cocco, M., Woesnner, J., Catalli, F., Wang, R. & Roth, F., 2009. Aftershock modeling based on uncertain stress calculations, *J. geophys. Res.,* **114,** B05309, doi:10.1029/2008JB006011.

Hainzl, S., Steacy, S. & Marsan, D., 2010. Seismicity models based on Coulomb stress calculations, *CORSSA,* **25,** doi:10.5078/corssa-32035809.

Holden, C., 2011. Kinematic source model of the 22 February 2011 Mw 6.2 Christchurch earthquake using strong motion data, *Seismol. Res. Lett,* **82,** 783–788.

Holden, C. & Beavan, J., 2012. Kinematic source studies of the ongoing (2010–2011) sequence of recent large earthquakes in Canterbury 2012, in the *Proceedings of NZSEE Conference*, Christchurch.

Ogata, Y., 1988. Statistical models for earthquake occurrences and residual analysis for point processes, *J. Am. Stat. Assoc.,* **83,** 9–27.

Ogata, Y. & Zhuang, J., 2006. Space-time ETAS models and an improved extension, *Tectonophysics,* **413,** 13–23.

Parsons, T., Toda, S., Stein, R.S., Barka, A. & Dieterich, J.H., 2000. Heightened odds of large earthquakes near Istanbul: an interaction-based probability calculation, *Science,* **288,** 661–665.

Rhoades, D.A. & Evison, F.F., 2004. Long-range earthquake forecasting with every earthquake a precursor according to scale, *Pure appl. Geophys.,* **161,** 47–72.

Rhoades, D., Schorlemmer, D., Gerstenberger, M., Christophersen, A., Zechar, J. & Imoto, M., 2011. Efficient testing of earthquake forecasting models, *Acta Geophys.,* **59,** 728–747.

Sibson, R.H., Ghisetti, F.C. & Ristau, J., 2011. Stress control of an evolving strike-slip fault system during the 2010–2011 Canterbury, New Zealand, earthquake sequence, *Seismol. Res. Lett.,* **82,** 824–832.

Steacy, S., Marsan, D., Nalbant, S.S. & McCloskey, J., 2004. Sensitivity of static stress calculations to the earthquake slip distribution, *J. geophys. Res.,* **109,** B04303, doi:10.1029/2002JB002365.

Steacy, S., Gomberg, J. & Cocco, M., 2005. Introduction to special section: stress transfer, earthquake triggering, and time-dependent seismic hazard, *J. geophys. Res.,* **110,** B05S01, doi:10.1029/2005JB003692.

Steacy, S., Jimenez, A. & Holden, C., 2013. Stress triggering and the Canterbury earthquake sequence, *Geophys. J. Int.*, doi:10.1093/gji/ggt380.

Toda, S., Stein, R.S., Richards-Dinger, K. & Bozkurt, S., 2005. Forecasting the evolution of seismicity in southern California: animations built on earthquake stress transfer, *J. geophys. Res.,* **110,** B05S16, doi:10.1029/2004JB003415.

Woessner, J. *et al.*, 2011. A retrospective comparative forecast test on the 1992 Landers sequence, *J. geophys. Res.,* **116,** B05305, doi:10.1029/2010JB007846.

Zechar, J., Gerstenberger, M. & Rhoades, D., 2010. Likelihood-based tests for evaluating space-rate-magnitude earthquake forecasts, *Bull. seism. Soc. Am.,* **100,** 1184–1195.

SUPPORTING INFORMATION

Additional Supporting Information may be found in the online version of this paper:

Figure S1: Pseudo prospective forecast rates for aftershocks following the February earthquake. As previously, top to bottom, left to right, the models are STEPC1, STEPC2, C-RS, and STEP.
Figure S2: Retrospective forecast rates for aftershocks following the February earthquake. As previously, top to bottom, left to right, the models are STEPC1, STEPC2, C-RS, and STEP.
Figure S3: Pseudo prospective forecast rates for aftershocks following the June earthquake. As previously, top to bottom, left to right, the models are STEPC1, STEPC2, C-RS, and STEP.
Figure S4: Retrospective forecast rates for aftershocks following the June earthquake. As previously, top to bottom, left to right, the models are STEPC1, STEPC2, C-RS, and STEP.
Figure S5: Pseudo prospective forecast rates for aftershocks following the December earthquake. As previously, top to bottom, left to right, the models are STEPC1, STEPC2, C-RS, and STEP.
Figure S6: Retrospective forecast rates for aftershocks following the December earthquake. As previously, top to bottom, left to right, the models are STEPC1, STEPC2, C-RS, and STEP.
Table S1. Values used in computing reference shear stress rate from reference seismicity rate.
Table S2. Frictional parameters used for Coulomb rate-state models.
(http://gji.oxfordjournals.org/lookup/suppl/doi:10.1093/gji/ggt404/-/DC1)

Please note: Oxford University Press is not responsible for the content or functionality of any supporting materials supplied by the authors. Any queries (other than missing material) should be directed to the corresponding author for the article.